SHEP-10-33
USM-TH-276

Fermiophobia in a Higgs Triplet Model

A.G. Akeroyd[a,b], Marco A. Díaz[c], Maximiliano A. Rivera[d], and Diego Romero[c]

[a] *Department of Physics and Center for Mathematics and Theoretical Physics, National Central University, Chungli, Taiwan 320, Taiwan.*

[b] *NExT Institute and School of Physics and Astronomy, University of Southampton Highfield, Southampton SO17 1BJ, United Kingdom.*

[c] *Departamento de Física, Pontificia Universidad Católica de Chile, Santiago 690441, Chile.*

[d] *Departamento de Física, Universidad Técnica Federico Santa María, Casilla 110-V, Valparaíso, Chile.*

(Dated: October 7, 2010)

A Fermiophobic Higgs boson can arise in models with an extended Higgs sector, such as models with scalars in an isospin triplet representation. In a specific model with a scalar triplet and spontaneous violation of lepton number induced by a scalar singlet field, we show that fermiophobia is not a fine-tuned situation, unlike in Two Higgs Doublet Models. We study distinctive signals of fermiophobia which can be probed at the LHC. For the case of a small Higgs mass a characteristic signal would be a moderate $B(H \to \gamma\gamma)$ accompanied by a large $B(H \to JJ)$ (where J is a Majoron), the latter being an invisible decay. For the case of a large Higgs mass there is the possibility of dominant $H \to ZZ, WW$ and suppressed $H \to JJ$ decay modes. In this situation, $B(H \to ZZ)$ is larger than $B(H \to WW)$, which differs from the SM prediction.

I. INTRODUCTION

The Standard Model (SM) of the electroweak and strong interactions is a very successful model, although the Higgs sector still needs to be probed by experiments. The LEP lower bound on the Higgs mass $m_H > 114.4$ GeV [1] has been complemented at Fermilab by ruling out the region between 160 and 170 GeV [2]. In the meantime the Large Hadron Collider (LHC) experiments ATLAS [3] and CMS [4] will soon join the search for the Higgs boson. In the SM, the Higgs sector is composed of one Higgs doublet under $SU(2)_L$, nevertheless, there is no reason why the Higgs sector may not be larger, and extensions are very often explored [5]. Higgs bosons in isospin triplet representations [6] have been studied, and are primarily motivated by a neutrino mass generation mechanism [7], for example via spontaneous violation of lepton number [8]. The phenomenology of the model has been well studied [9], and more recently, renewed attention has been given to the detection prospects of the doubly and singly charged scalars at the LHC [10]

(for earlier studies see e.g. [11]).

Fermiophobic Higgs bosons [12], *i.e.*, neutral Higgs bosons with negligible couplings to fermions, can arise in models with Higgs triplets, as well as in two Higgs doublet models (2HDM). A Higgs boson of this type, denoted by h_f, would dominantly decay via $h_f \to \gamma\gamma$ for $m_f \lesssim 95$ GeV, and via $h_f \to W^+W^-$ and $h_f \to ZZ$ for $m_f \gtrsim 95$ GeV, for a Higgs with SM like couplings to gauge bosons [13]. In the latter case, the decay rates satisfy $\Gamma(h_f \to W^+W^-)/\Gamma(h_f \to ZZ) \gtrsim 2$, in the region of large Higgs mass [14].

In this article we study the appearance of fermiophobic Higgs bosons in a particular Higgs Triplet Model (HTM) that includes a singlet, a doublet and a triplet Higgs field, the so-called "123 models". These models are characterized by a spontaneous violation of a global $U(1)$ symmetry through a vacuum expectation value of a $SU(2) \times U(1)$ Higgs singlet $\langle\sigma\rangle$. Therefore, this broken symmetry produces a massless Goldstone Boson called a Majoron (J). Within this model we show that fermiophobia is not a fine-tuned situation as in the 2HDM. In fact, the model has a tendency towards fermiophobia mainly due to the hierarchy of the three vacuum expectation values. Furthermore, we emphasize a scenario in which the decay of the fermiophobic Higgs boson to Majorons via $h \to JJ$ is partially suppressed, thereby allowing branching ratios of a fermiophobic Higgs into gauge bosons which can be probed by the LHC. Our work is organized as follows. In section II we introduce the Higgs Triplet Model and in Section III the scenario of fermiophobia with Majoron suppression is described. In section IV the decays of the fermiophobic Higgs boson are discussed, with phenomenology studied in section V. Conclusions are contained in section VI.

II. HIGGS TRIPLET MODEL

The Higgs Triplet Model (HTM) which we will study [9], includes a complex triplet Higgs field Δ with lepton number $L = -2$ and hypercharge $Y = 2$, a complex doublet Higgs field ϕ, with lepton number $L = 0$ and hypercharge $Y = -1$,

$$\Delta = \begin{bmatrix} \Delta^0 & \Delta^+/\sqrt{2} \\ \Delta^+/\sqrt{2} & \Delta^{++} \end{bmatrix}, \qquad \phi = \begin{bmatrix} \phi^0 \\ \phi^- \end{bmatrix}, \tag{1}$$

and a complex singlet Higgs field σ, with lepton number $L = 2$ and hypercharge $Y = 0$. The model without the singlet field has received much attention recently [10], and we note the phenomenology of the charged scalars (doubly and singly) at the LHC is essentially identical in both models.

A. Higgs Potential and Mass Spectrum

The scalar potential can be written as follows:

$$\begin{aligned} V(\phi,\Delta,\sigma) \;=\; & \mu_1^2\sigma^\dagger\sigma + \mu_2^2\phi^\dagger\phi + \mu_3^2\,\mathrm{tr}(\Delta^\dagger\Delta) + \lambda_1(\phi^\dagger\phi)^2 + \lambda_2[\mathrm{tr}(\Delta^\dagger\Delta)]^2 \\ & +\lambda_3\phi^\dagger\phi\,\mathrm{tr}(\Delta^\dagger\Delta) + \lambda_4\,\mathrm{tr}(\Delta^\dagger\Delta\Delta^\dagger\Delta) + \lambda_5(\phi^\dagger\Delta^\dagger\Delta\phi) \\ & +\beta_1(\sigma^\dagger\sigma)^2 + \beta_2(\phi^\dagger\phi)(\sigma^\dagger\sigma) + \beta_3\,\mathrm{tr}(\Delta^\dagger\Delta)\sigma^\dagger\sigma \\ & -\kappa(\phi^T\Delta\phi\sigma + \mathrm{h.c.}). \end{aligned} \tag{2}$$

where μ_i^2, $i = 1, 2, 3$, are mass squared parameters, λ_i, $i = 1, ..., 5$ are dimensionless couplings not related to the singlet, β_i, $i = 1, 2, 3$ are dimensionless couplings related to the singlet, and κ is a dimensionless coupling that mixes all three Higgs fields.

The electroweak symmetry is spontaneously broken when the neutral components of the Higgs fields acquire vacuum expectation values v_i, $i = 1, 2, 3$. We shift the Higgs fields in the following way,

$$\begin{aligned} \sigma &= \frac{v_1}{\sqrt{2}} + \frac{R_1 + iI_1}{\sqrt{2}} \\ \phi^0 &= \frac{v_2}{\sqrt{2}} + \frac{R_2 + iI_2}{\sqrt{2}} \\ \Delta^0 &= \frac{v_3}{\sqrt{2}} + \frac{R_3 + iI_3}{\sqrt{2}} \end{aligned} \tag{3}$$

finding minimization conditions, or tree-level tadpole equations, given by,

$$V_{lineal} = t_1R_1 + t_2R_2 + t_3R_3 = 0\,, \tag{4}$$

where

$$\begin{aligned} t_1 &= v_1(\mu_1^2 + \beta_1v_1^2 + \tfrac{1}{2}\beta_2v_2^2 + \tfrac{1}{2}\beta_3v_3^2) - \tfrac{1}{2}\kappa v_3v_2^2 \\ t_2 &= v_2(\mu_2^2 + \lambda_1v_2^2 + \tfrac{1}{2}\lambda_3v_3^2 + \tfrac{1}{2}\lambda_5v_3^2 + \tfrac{1}{2}\beta_2v_1^2 - \tfrac{1}{2}\kappa v_1v_3) \\ t_3 &= v_3(\mu_3^2 + \lambda_2v_3^2 + \tfrac{1}{2}\lambda_3v_2^2 + \lambda_4v_3^2 + \tfrac{1}{2}\lambda_5v_2^2 + \tfrac{1}{2}\beta_3v_1^2) - \tfrac{1}{2}\kappa v_1v_2^2. \end{aligned} \tag{5}$$

In ref. [9] cases where different vacuum expectation values are equal to zero are analyzed, but these scenarios are not relevant for our purposes. In the following we assume all vev's are non zero.

The quadratic potential can be written as follows,

$$V_{quadratic} = \tfrac{1}{2}\Big[R_1, R_2, R_3\Big]\boldsymbol{M}_R^2 \begin{bmatrix} R_1 \\ R_2 \\ R_3 \end{bmatrix} + \tfrac{1}{2}\Big[I_1, I_2, I_3\Big]\boldsymbol{M}_I^2 \begin{bmatrix} I_1 \\ I_2 \\ I_3 \end{bmatrix} + \Big[\phi^-, \Delta^-\Big]\boldsymbol{M}_+^2 \begin{bmatrix} \phi^+ \\ \Delta^+ \end{bmatrix} + m_{\Delta^{++}}^2 \Delta^{++}\Delta^{--} \tag{6}$$

The CP-even neutral Higgs mass matrix is given by,

$$\boldsymbol{M}_R^2 = \begin{bmatrix} 2\beta_1 v_1^2 + \frac{1}{2}\kappa v_2^2 \frac{v_3}{v_1} + \frac{t_1}{v_1} & \beta_2 v_1 v_2 - \kappa v_2 v_3 & \beta_3 v_1 v_3 - \frac{1}{2}\kappa v_2^2 \\ \beta_2 v_1 v_2 - \kappa v_2 v_3 & 2\lambda_1 v_2^2 + \frac{t_2}{v_2} & (\lambda_3 + \lambda_5) v_2 v_3 - \kappa v_1 v_2 \\ \beta_3 v_1 v_3 - \frac{1}{2}\kappa v_2^2 & (\lambda_3 + \lambda_5) v_2 v_3 - \kappa v_1 v_2 & 2(\lambda_2 + \lambda_4) v_3^2 + \frac{1}{2}\kappa v_2^2 \frac{v_1}{v_3} + \frac{t_3}{v_3} \end{bmatrix} \tag{7}$$

where we have eliminated the mass parameters μ_i^2 using the tadpole equations. This mass matrix is diagonalized by an orthogonal matrix O_R, which can be parametrized with three angles,

$$\begin{aligned} O_R &= \begin{bmatrix} 1 & 0 & 0 \\ 0 & c_{23} & s_{23} \\ 0 & -s_{23} & c_{23} \end{bmatrix} \begin{bmatrix} c_{13} & 0 & s_{13} \\ 0 & 1 & 0 \\ -s_{13} & 0 & c_{13} \end{bmatrix} \begin{bmatrix} c_{12} & s_{12} & 0 \\ -s_{12} & c_{12} & 0 \\ 0 & 0 & 1 \end{bmatrix} \\ &= \begin{bmatrix} c_{13}c_{12} & c_{13}s_{12} & s_{13} \\ -c_{23}s_{12} - s_{23}s_{13}c_{12} & c_{23}c_{12} - s_{23}s_{13}s_{12} & s_{23}c_{13} \\ s_{23}s_{12} - c_{23}s_{13}c_{12} & -s_{23}c_{12} - c_{23}s_{13}s_{12} & c_{23}c_{13} \end{bmatrix} \end{aligned} \tag{8}$$

where $s_{12} = \sin\theta_{12}$, $c_{12} = \cos\theta_{12}$, and similarly for the other two angles θ_{13} and θ_{23}.

The CP-odd neutral Higgs mass matrix is,

$$\boldsymbol{M}_I^2 = \begin{bmatrix} \frac{1}{2}\kappa v_2^2 \frac{v_3}{v_1} + \frac{t_1}{v_1} & \kappa v_2 v_3 & \frac{1}{2}\kappa v_2^2 \\ \kappa v_2 v_3 & 2\kappa v_1 v_3 + \frac{t_2}{v_2} & \kappa v_1 v_2 \\ \frac{1}{2}\kappa v_2^2 & \kappa v_1 v_2 & \frac{1}{2}\kappa v_2^2 \frac{v_1}{v_3} + \frac{t_3}{v_3} \end{bmatrix}. \tag{9}$$

Clearly, this mass matrix has two zero eigenvalues, of which one is unphysical and corresponds to the neutral Goldstone boson. The other one is physical and corresponds to the Majoron J. The third eigenvalue is the CP-odd neutral Higgs A, and has a mass given by,

$$m_A^2 = \frac{\kappa}{2}\left(\frac{v_1 v_2^2}{v_3} + \frac{v_2^2 v_3}{v_1} + 4 v_1 v_3\right) \tag{10}$$

As one can see, a value for $\kappa \neq 0$ is essential in our model in order to have a massive CP-odd Higgs boson.

The charged Higgs mass matrix, given by

$$\boldsymbol{M}_+^2 = \tfrac{1}{2}(\kappa v_1 v_2 - \tfrac{1}{2}\lambda_5 v_2 v_3) \begin{bmatrix} 2v_3/v_2 & -\sqrt{2} \\ -\sqrt{2} & v_2/v_3 \end{bmatrix}. \tag{11}$$

also has a zero eigenvalue, corresponding to the charged Goldstone boson. It is diagonalized by an orthogonal matrix O_+ such that $O_+ \, \boldsymbol{M}_+^2 \, O_+^T = \mathrm{diag}(m_{H^+}^2, 0)$. The rotation matrix is,

$$O_+ = \begin{bmatrix} c_+ & s_+ \\ -s_+ & c_+ \end{bmatrix} = \frac{1}{\sqrt{v_2^2 + 2v_3^2}} \begin{bmatrix} \sqrt{2}v_3 & -v_2 \\ v_2 & \sqrt{2}v_3 \end{bmatrix} \tag{12}$$

where $s_+ = \sin\theta_+$, $c_+ = \cos\theta_+$, and θ_+ is the angle of rotation. The massive eigenvalue is the singly charged Higgs boson, with a mass,

$$m_{H^+}^2 = \frac{1}{2}\left(\kappa\frac{v_1}{v_3} - \frac{1}{2}\lambda_5\right)(v_2^2 + 2v_3^2) \tag{13}$$

Finally, the doubly charged Higgs boson has the following mass,

$$m_{\Delta^{++}}^2 = \tfrac{1}{2}\kappa\frac{v_1 v_2^2}{v_3} - \tfrac{1}{2}\lambda_5 v_2^2 - \lambda_4 v_3^2 \tag{14}$$

B. Gauge Sector

The kinetic terms of the Higgs fields are,

$$\mathcal{L}_{\mathrm{kinetic}} = (D_\mu\phi)^\dagger(D^\mu\phi) + \mathrm{Tr}\left[(D_\mu\Delta)^\dagger(D^\mu\Delta)\right] + \partial_\mu\sigma^\dagger\partial^\mu\sigma \tag{15}$$

where the covariant derivatives can be written as,

$$D_\mu = \partial_\mu + ig\mathbf{T}_a W_\mu^a + i\tfrac{1}{2}g'\mathbf{Y}B_\mu \tag{16}$$

where the action of the isospin and hypercharge operators $\mathbf{T}$ and $\mathbf{Y}$ on the Higgs doublet and triplet is

$$\begin{aligned} \mathbf{T}_a\phi &= \tfrac{1}{2}\tau_a\phi\,, & \mathbf{T}_a\Delta &= -\tfrac{1}{2}\tau_a^*\Delta - \tfrac{1}{2}\Delta\tau_a \\ \mathbf{Y}\phi &= -\phi\,, & \mathbf{Y}\Delta &= 2\Delta \end{aligned} \tag{17}$$

Gauge bosons receive contributions to their masses from the the doublet and triplet. After these scalar fields acquire vacuum expectation values, we find,

$$m_W^2 = \frac{1}{4}g^2(v_2^2 + 2v_3^2)\,, \qquad m_Z^2 = \frac{1}{4}(g^2 + g'^2)(v_2^2 + 4v_3^2) \tag{18}$$

which leads to the following ρ-parameter at tree-level,

$$\rho = 1 - \frac{2v_3^2}{v_2^2 + 4v_3^2} \tag{19}$$

The experimental measurement of ρ is given by $\rho = 1.0002^{+0.0007}_{-0.0004}$, and this restricts the value of the triplet vev to be smaller than a few GeV. Nevertheless, in order to satisfy stringent bounds from astrophysics, we will work with $v_3 < 0.35$ GeV [9]. From eq. (10) we see that the small value for v_3 implies in turn a small value for the coupling κ in order to have a CP-odd Higgs mass m_A below 1 TeV. Another consequence of the small value for v_3 is that the vacuum expectation value of the Higgs doublet v_2 will be very close to 246 GeV, as indicated by the gauge bosons masses in eq. (18).

III. FERMIOPHOBIA AND MAJORON SUPPRESSION

Fermiophobia was first introduced in [12], where it was stressed that the mechanism for the generation of fermion masses could be independent of the mechanism for the generation of the masses of the gauge bosons (e.g. a 2HDM in which the fermions receive mass from just one vacuum expectation value, while the gauge bosons receive mass from both).

We investigate the possibility that the lightest CP-even Higgs boson is fermiophobic, in which case the conventional decay modes, $H_1^0 \to b\overline{b}, \tau^-\tau^+$, are suppressed. In addition, we study the singlet content of this Higgs boson, looking for cases in which the fermiophobic Higgs has a suppressed mixing with the singlet field, a situation which we call "Majoron suppression". If the fermiophobic Higgs has a large mixing with the singlet, it will decay mainly into two Majorons, which leads to a missing energy signature. In this paper we focus on signatures of fermiophobia which are visible in detectors.

We start by doing a general scan of the parameter space as follows:

$$\begin{aligned} 0.5\,\mathrm{GeV} < v_1 < 1\,\mathrm{TeV}\,, \qquad v_2 = 246\,\mathrm{GeV}\,, \qquad v_3 < 0.35\,\mathrm{GeV}\,, \\ 0 < \kappa < 0.1\,, \qquad |\beta_{1,2,3}| < 4\,, \qquad |\lambda_{1\ldots5}| < 4\,. \end{aligned} \tag{20}$$

Our aim is to see how large the parameter space is for fermiophobia and Majoron suppression for the lightest CP-even Higgs boson. In addition to eq. (20), we respect the current experimental limits for the masses of A^0, $H^\pm$, and $\Delta^{\pm\pm}$ ($m_A > 90$ GeV, $m_{H^+} > 80$ GeV, $m_{\Delta^{++}} > 136$ GeV), and we also require $90 < m_{H_1} < 300$ GeV.

In the left frame of Fig. 1 we show a frequency histogram from which one can see the values of the matrix element O_R^{12} (see eq. (8)), with no other restriction on the parameters in the Lagrangian, except for a correct minimization of the scalar potential. In this plot we see the rather unexpected result that a sharp maximum is obtained at $O_R^{12} = 0$, indicating a high concentration of points in the fermiophobic region. Therefore we conclude that fermiophobia is not a fine-tuned scenario in this model.

In Table I we show the fraction of points from the general scan of the parameter space (defined by

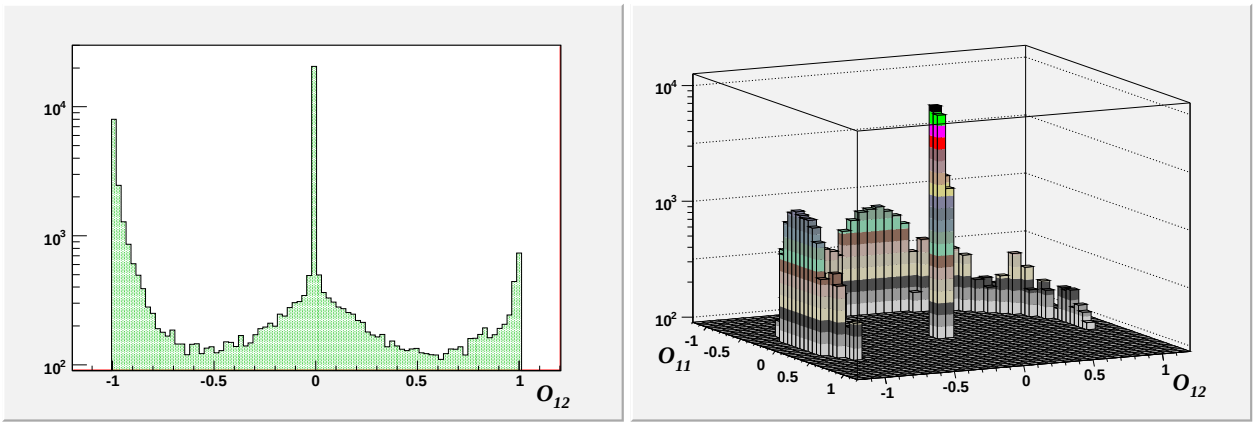

FIG. 1: *Frequency histogram for O_R^{12} (left frame) and O_R^{11}-O_R^{12} (right frame) in a general scan of parameter space.*

eq. (20)) that lie in a given region around the exact fermiophobic point $|O_R^{12}| = 0$. Clearly it is not necessary to deviate too much from $|O_R^{12}| = 0$ in order to encapsulate an important number of the points in parameter space. In other words, the model has a "preference" for fermiophobia. The reason for this is that the CP-even neutral mass matrix in eq. (7) has diagonal elements which are much larger than the non-diagonal elements in a large region of parameter space, making O_R^{12} naturally small. This feature is present in our model due to both the hierarchy of the three vacuum expectation values and the smallness of the κ coupling.

Fraction of Scan	Max. $\lvert O_R^{12}\rvert$ value
45%	0,070
40%	0,0086
30%	0,0014
20%	0,00056
10%	0,00019

TABLE I: Fraction of points in the general scan of the parameter space that are within a given region around the point of exact fermiophobia defined by $|O_R^{12}| = 0$.

In the right frame of Fig. 1 we show a two-dimensional frequency histogram in the plane $O_R^{11} - O_R^{12}$, within the same scan as before. The peak around $O_R^{11} = O_R^{12} = 0$ (or equivalently $O_R^{13} = 1$) corresponds to a fermiophobic Higgs with suppressed couplings to the Majoron, implying that the visible decay modes of this Higgs boson are not suppressed. The concentration of parameter space points around $O_R^{13} = 1$ is again due to the hierarchy of vacuum expectation values.

In Table II we display the fraction of points within a given region around the exact fermiophobic and Majoron suppressed case, defined by $|O_R^{13}| = 1$. It is surprising how little deviation from this point is nec-

Fraction of Scan	Min. $\lvert O_R^{13}\rvert$ value
41.5%	0.9
41.0%	0.999
36.6%	0.99999
27.8%	0.999999
14.0%	0.9999999

TABLE II: Fraction of points in the general scan of the parameter space that are within a given region around the point of exact fermiophobia and Majoron suppression defined by $|O_R^{13}| = 1$.

essary to find a large fraction of the scan points around the fermiophobic and Majoron suppressed situation, indicating that it is not a fine-tuned case in this model.

A. Imposing Fermiophobia in the CP-even Higgs Sector

We are interested in the possibility of having a light CP-even neutral Higgs boson with suppressed couplings to fermions (fermiophobia). A light fermiophobic Higgs boson is characterized by $O_R^{12} = c_{13}s_{12} = 0$, since it is mainly the Higgs doublet ϕ which couples to fermions (the triplet coupling to the fermions is suppressed). With the condition $s_{12} = 0$ we find general fermiophobia. The diagonalizing matrix in this case is,

$$O_R = \begin{bmatrix} \pm c_{13} & 0 & s_{13} \\ \mp s_{23}\, s_{13} & \pm c_{23} & s_{23}\, c_{13} \\ \mp c_{23}\, s_{13} & \mp s_{23} & c_{23}\, c_{13} \end{bmatrix} \tag{21}$$

where $\pm$ corresponds to $\mathrm{sign}(c_{12})$. The diagonalized CP-even Higgs mass matrix is given by $(\mathbf{M}_R^2)_{diag} = O_R \mathbf{M}_R^2 O_R^T$, and implies the following consistency conditions,

$$\begin{aligned} \mathbf{M}_{R11}^2 &= \mp\left(\frac{s_{13}}{c_{13}} - \frac{c_{13}}{s_{13}}\right)\mathbf{M}_{R13}^2 + \mathbf{M}_{R33}^2 \\ \mathbf{M}_{R12}^2 &= \mp\frac{s_{13}}{c_{13}}\mathbf{M}_{R23}^2 \\ \mathbf{M}_{R22}^2 &= \mp\frac{s_{13}}{c_{13}}\mathbf{M}_{R13}^2 \mp \left(\frac{s_{23}}{c_{23}} - \frac{c_{23}}{s_{23}}\right)\frac{1}{c_{13}}\mathbf{M}_{R23}^2 + \mathbf{M}_{R33}^2 \end{aligned} \tag{22}$$

which allow us to eliminate three parameters of the potential in favour of the three angles in eq. (8). These three parameters are chosen as,

$$\begin{aligned} \beta_1 &= \frac{1}{2v_1^2}\left(\mathbf{M}^2_{R11} - \tfrac{1}{2}\kappa v_2^2 \frac{v_3}{v_1}\right) \\ \beta_2 &= \frac{1}{v_1 v_2}\left(\mathbf{M}^2_{R12} + \kappa v_2 v_3\right) \\ \lambda_1 &= \frac{1}{2v_2^2}\mathbf{M}^2_{R22} \end{aligned} \tag{23}$$

with the above expressions found from eq. (7).

We do a scan of parameter space, imposing fermiophobia in the way just described. The free parameters are varied according to,

$$\begin{aligned} 0.5\,\mathrm{GeV} < v_1 < 1\,\mathrm{TeV}\,, \qquad & v_2 = 246\,\mathrm{GeV}\,, \qquad & v_3 < 0.35\,\mathrm{GeV}\,, \\ 0 < \kappa < 0.1\,, \qquad & |\beta_3| < 4\,, \qquad & |\lambda_{2\ldots5}| < 4\,, \\ \theta_{12} = 0\,, \qquad & 0 < \theta_{13} < 2\pi\,, \qquad & 0 < \theta_{23} < 2\pi\,. \end{aligned} \tag{24}$$

checking that β_1, β_2, and λ_1 have all an absolute value smaller than 4.

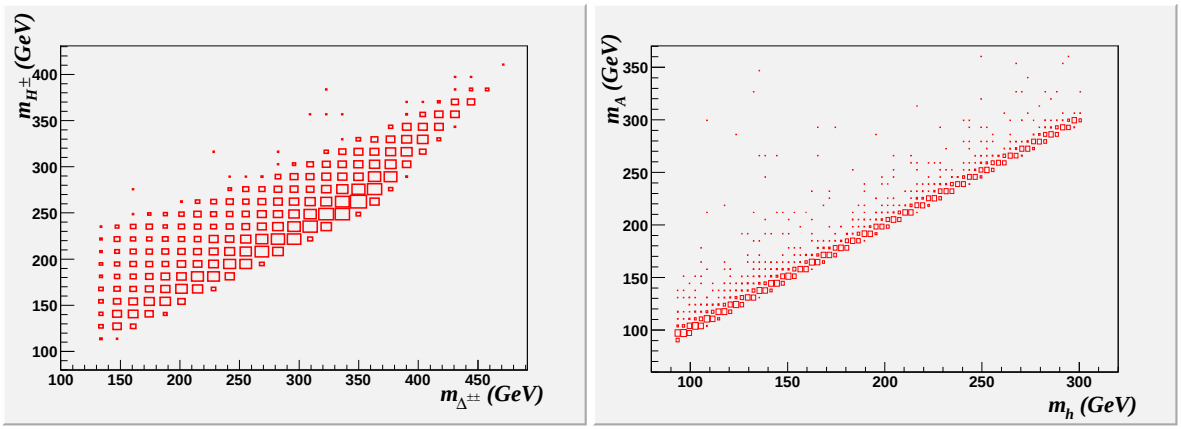

FIG. 2: *Charged Higgs and doubly-charged Higgs boson masses as a function of the fermiophobic Higgs mass.*

In order to study the masses of the scalars in the pure fermiophobic limit, in Fig. 2 we show a scatter plot of m_{H^+} and $m_{\Delta^{++}}$ (left frame), and a scatter plot of m_A and m_{H_1} (right frame), resulting from the scan. The correlation between the singly and doubly charged Higgs boson masses is understood from the small value of the triplet vev, which implies that the charged Higgs bosons satisfy,

$$\begin{aligned} m^2_{H^+} &\approx m^2_A - \tfrac{1}{4}\lambda_5 v_2^2 \\ m^2_{\Delta^{++}} &\approx m^2_A - \tfrac{1}{2}\lambda_5 v_2^2 \end{aligned} \tag{25}$$

This indicates that the singly charged Higgs boson mass lies in a narrower region than the doubly charged Higgs mass, and this effect can be seen in the figures. Note that this implies,

$$m^2_{H^+} \approx \tfrac{1}{2}(m^2_A + m^2_{\Delta^{++}}) \tag{26}$$

which is a very good approximation up to order $\mathcal{O}(v_3)$.

The correlation between the CP-odd Higgs mass m_A and the lightest CP-even Higgs mass m_{H_1} seen in the right frame of Fig. 2 is explained by inspecting the CP-even Higgs boson mass matrix in eq. (7), and the CP-odd mass in eq. (10). Due to the hierarchy of vevs we see that,

$$(\mathbf{M}^2_R)_{33} \approx m^2_A \approx \frac{\kappa v_1 v_2^2}{2v_3} \sim m^2_{H_1} \tag{27}$$

where the last relation comes from the fact that most of the time the CP-even Higgs mass matrix is nearly diagonal, with the $(\mathbf{M}^2_R)_{33}$ element being the smallest.

Another point we wish to emphasize here is the relation between the couplings of the fermiophobic Higgs boson to charged scalars and to gauge bosons. In the left frame of Fig. 3 we show the relation

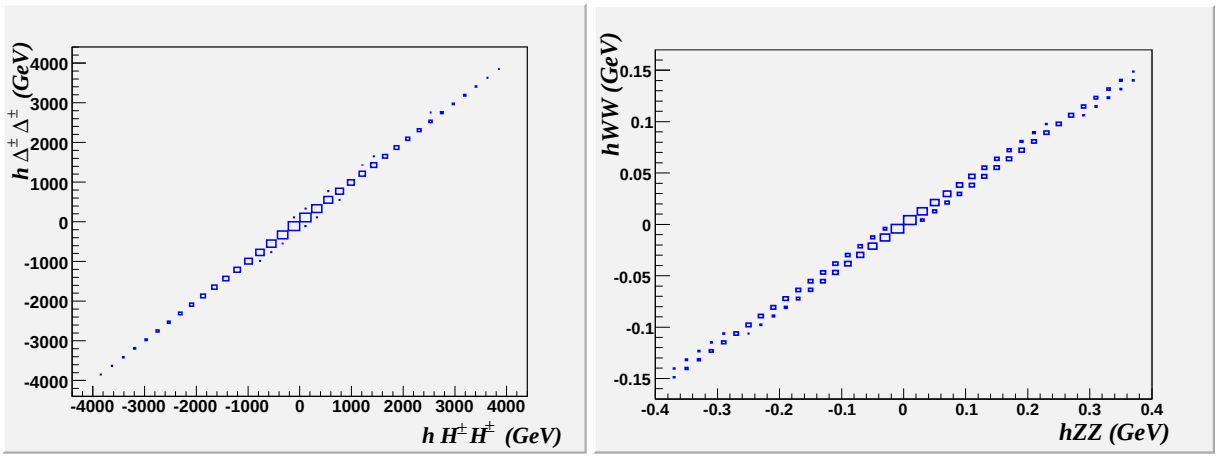

FIG. 3: *Fermiophobic Higgs boson couplings to a pair of charged Higgs (left) and to a pair of gauge bosons(right).*

between the couplings $h_f\Delta^{++}\Delta^{--}$ and $h_f H^+H^-$ (see appendix A for Feynman rules), when we vary all parameters as indicated in eq. (24). The couplings are clearly proportional to each other, as can be inferred from the Feynman rules, which in the fermiophobic case satisfy,

$$\frac{\lambda(h_f\Delta^{++}\Delta^{--})}{\lambda(h_f H^+H^-)} = 1 + \mathcal{O}(v_3) \tag{28}$$

These couplings can have a magnitude as large as 4 TeV, although in most of the parameter space they are $\lesssim 300$ GeV. Similarly, in the right frame of Fig. 3 we plot the relation between the couplings $h_f W^+W^-$

and $h_f ZZ$.

$$\frac{\lambda(h_1 W^+W^-)}{\lambda(h_1 ZZ)} = c_W^2 \frac{2v_3 O_R^{13} + v_2 O_R^{12}}{4v_3 O_R^{13} + v_2 O_R^{12}} \tag{29}$$

and if we take the exact fermiophobic limit we get,

$$\frac{\lambda(h_f W^+W^-)}{\lambda(h_f ZZ)} \longrightarrow \tfrac{1}{2} c_W^2 \tag{30}$$

which is half the value for a SM Higgs boson. This has implications that will be evaluated in the next sections. Note that this limit changes drastically with a small but non-zero value for O_R^{12}. Notice also that the couplings $h_f W^+W^-$ and $h_f ZZ$ are much smaller in this fermiophobic limit than the equivalent SM couplings.

Within the same scan of parameter space in the fermiophobic scenario given by eq. (24) we explore in Fig. 4 the magnitude of couplings with and without a Majoron. In the left frame of Fig. 4 we have the relation between the $\lambda(h_f ZJ)$ and $\lambda(h_f ZA)$ couplings. The $\lambda(h_f ZA)$ coupling can be large, but it is not relevant for the decay of a fermiophobic Higgs, since m_{h_f} is rarely larger than $m_Z + m_A$, as indicated in Fig. 2. On the contrary, the coupling $\lambda(h_f ZJ)$ is very small and irrelevant for production of a fermiophobic Higgs boson. Nevertheless, the decay $h_f \to ZJ$ is possible and it is characterized by missing energy. We evaluate its branching ratio in the next section.

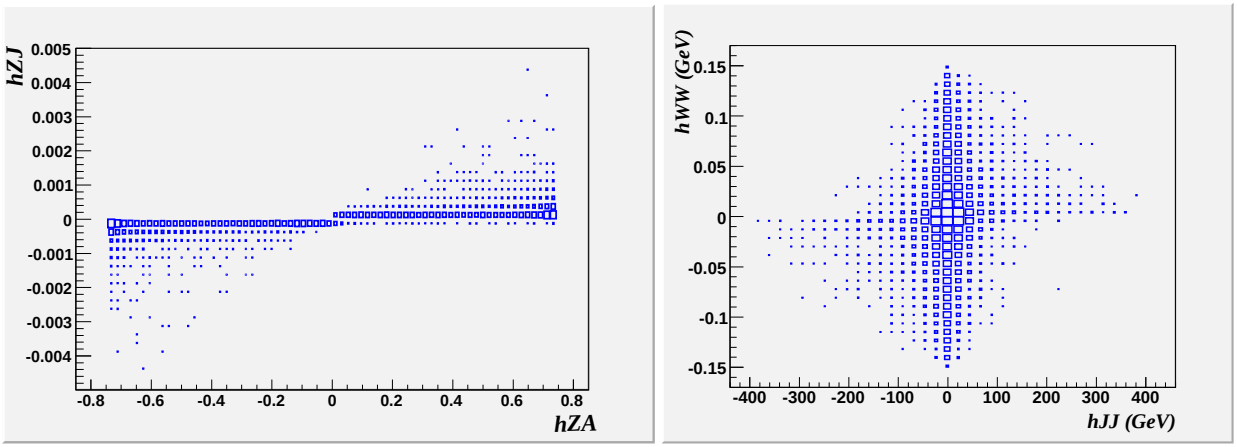

FIG. 4: *Relation between couplings with and without Majoron in the Fermiophobic scenario.*

In the right frame of Fig. 4 we see the relation between the $\lambda(h_f JJ)$ and $\lambda(h_f WW)$ couplings. The coupling $\lambda(h_f WW)$ is diminished compared to the value in the SM, implying that the decay rate $h_f \to WW$ is small. Nevertheless its branching ratio, together with the comparable BR for $h_f \to ZZ$, will dominate unless the invisible decay $h_f \to JJ$ is large. This decay is controlled by the coupling $\lambda(h_f JJ)$, also displayed in the right frame of Fig. 4. We see that this coupling can be large, in which case the fermiophobic Higgs will be invisible. In this scenario, one has to look for the second lightest Higgs boson.

B. Imposing Fermiophobia and Majoron Suppression

We impose exact fermiophobia and Majoron suppression by fixing the value of $\cos\theta_{13} = c_{13} = 0$ in eq.(8). The diagonalizing matrix in this case is,

$$O_R = \begin{bmatrix} 0 & 0 & \pm 1 \\ -c_{23}s_{12} \mp s_{23}c_{12} & c_{23}c_{12} \mp s_{23}s_{12} & 0 \\ s_{23}s_{12} \mp c_{23}c_{12} & -s_{23}c_{12} \mp c_{23}s_{12} & 0 \end{bmatrix} = \begin{bmatrix} 0 & 0 & \pm 1 \\ -\sin\theta & \cos\theta & 0 \\ \mp\cos\theta & \mp\sin\theta & 0 \end{bmatrix} \tag{31}$$

where $\pm$ corresponds to $\mathrm{sign}(s_{13})$, and $\theta \equiv \theta_{12} \pm \theta_{23}$ is introduced as a new independent parameter. The last definition indicates that only one angle controls the rotation matrix in this scenario.

The diagonalized CP-even Higgs mass matrix $(\mathbf{M}_R^2)_{diag} = O_R \mathbf{M}_R^2 O_R^T$, implies,

$$\begin{aligned} \mathbf{M}_{R13}^2 &= 0 \\ \mathbf{M}_{R23}^2 &= 0 \\ \mathbf{M}_{R12}^2 &= \frac{1}{2}(\mathbf{M}_{R11}^2 - \mathbf{M}_{R22}^2)\tan 2\theta \end{aligned} \tag{32}$$

From these equations we eliminate the following parameters from the list of independent parameters given in eq. (20),

$$\begin{aligned} \beta_3 &= \frac{\kappa v_2^2}{2v_1 v_3} \\ \kappa &= (\lambda_3 + \lambda_5)\frac{v_3}{v_1} \\ \beta_2 &= \kappa\frac{v_3}{v_1} + \frac{1}{2v_1 v_2}\Big(2\beta_1 v_1^2 + \frac{1}{2}\kappa v_2^2\frac{v_3}{v_1} - 2\lambda_1 v_2^2\Big)\tan 2\theta \end{aligned} \tag{33}$$

We do a scan of the parameter space, imposing fermiophobia and Majoron suppression. The free parameters are varied according to,

$$\begin{aligned} 0.5\,\mathrm{GeV} < v_1 < 1\,\mathrm{TeV}\,, \qquad v_2 = 246\,\mathrm{GeV}\,, \qquad v_3 < 0.35\,\mathrm{GeV}\,, \\ |\beta_1| < 4\,, \qquad |\lambda_{1\ldots5}| < 4\,, \qquad 0 < \theta < 2\pi\,. \end{aligned} \tag{34}$$

checking that β_2, β_3 and κ have values smaller than 4.

First we notice the clear dependence of the doubly charged Higgs mass $m_{\Delta^{++}}$ on λ_3, shown in Fig. 5. This dependence is easily understood from the expression for the mass $m_{\Delta^{++}}$ in eq. (14), which after replacing κ from eq. (33) transforms into,

$$m_{\Delta^{++}}^2 \approx \frac{1}{2}\lambda_3 v_2^2 - \lambda_4 v_3^2 \tag{35}$$

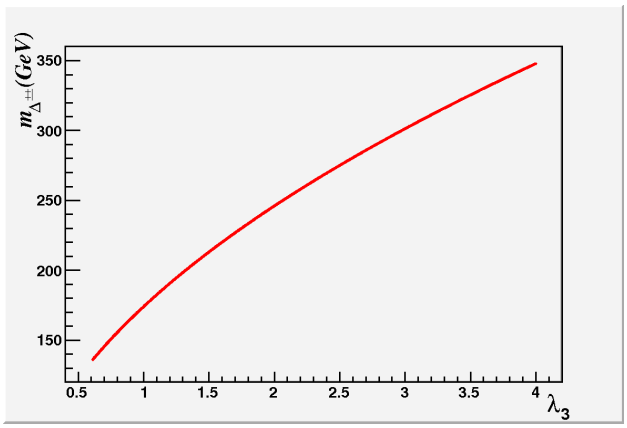

FIG. 5: *Doubly charged Higgs mass dependence on λ_3 coupling in the Fermiophobic and Majoron suppressed scenario.*

with the equality holding in the exact fermiophobic and Majoron suppression scenario. Since $v_3 \ll v_2$, this relation would enable a direct determination of λ_3 from experiments. Note also that the relation in eq. (26) is valid also in the fermiophobic plus Majoron suppression scenario (since it is a special case of the fermiophobic case), thus providing a measurement that could validate or refute the model.

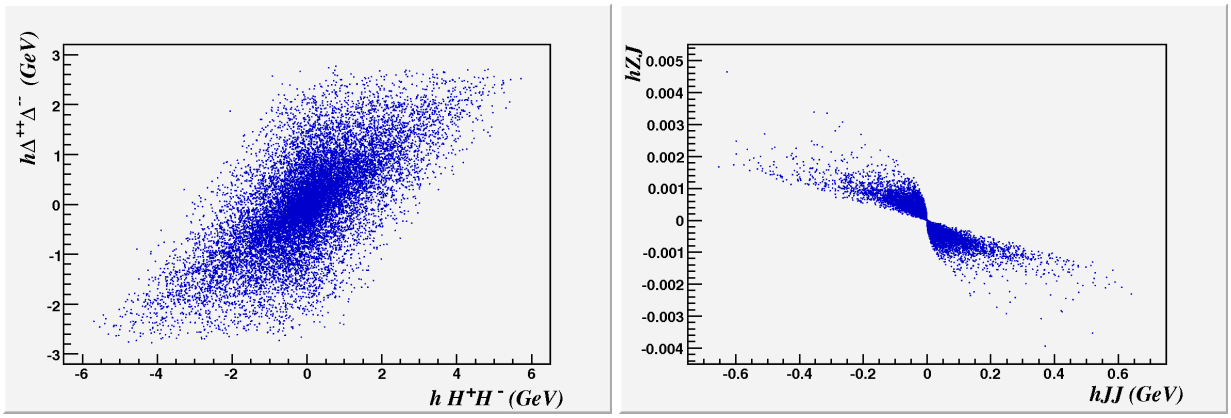

FIG. 6: *Relation between couplings with and without Majoron in the Fermiophobic and Majoron suppressed scenario.*

In the left frame of Fig. 6 we plot the relation between the fermiophobic Higgs couplings to a pair of charged Higgs $\lambda(h_f H^+ H^-)$ and to a pair of doubly charged Higgs bosons $\lambda(h_f \Delta^{++}\Delta^{--})$. Clearly, the suppression of the Majoron component in the fermiophobic Higgs reduces dramatically the value of these couplings (compare with the left frame of Fig. 3), which are important for the decay rate for the $h_f \to \gamma\gamma$ mode.

In the right frame of Fig. 6 we study couplings that involve one or two Majorons. To be more specific, we see the relation between $\lambda(h_f ZJ)$ and $\lambda(h_f JJ)$, the first one corresponding to h_f decay with missing

energy, and the second one corresponding to an invisible decay. The coupling $\lambda(h_f ZJ)$ maintains its magnitude compared with the previous scenario, but $\lambda(h_f JJ)$ is much smaller, an expected effect since this scenario is defined by a null singlet component in h_f.

IV. FERMIOPHOBIC HIGGS BOSON DECAYS

A fermiophobic Higgs boson will have four main decay modes, two of them into a pair of massive gauge bosons, $h_f \to W^+W^-$ and $h_f \to ZZ$, where one or two of the gauge bosons may be off-shell depending on the Higgs mass, and the other two into one or two photons $h_f \to \gamma\gamma$ and $h_f \to \gamma Z$, decays which are generated at one-loop [15].

In the later case, W gauge boson contribute to the one-loop generated decay with the graphs,

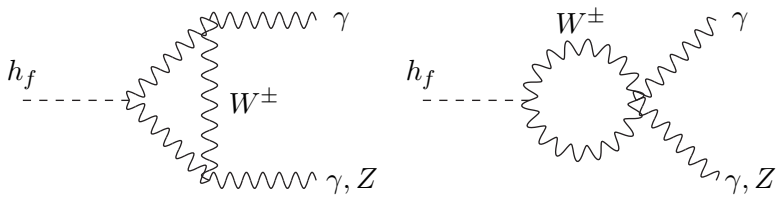

present already in the SM. These graphs are complemented in our model with singly and doubly charged Higgs bosons,

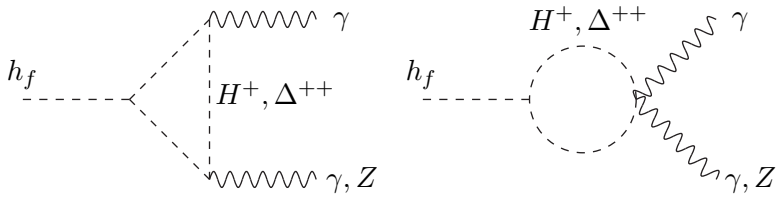

The decay rate for $h_f \to \gamma\gamma$ is given by,

$$\Gamma(h_f \to \gamma\gamma) = \frac{\alpha^2 g^2}{1024\pi^3}\frac{m_{h_f}^3}{m_W^2}|F_0(\tau_H)\,\tilde{g}_{hHH} + 4F_0(\tau_\Delta)\,\tilde{g}_{h\Delta\Delta} - F_1(\tau_W)\,\tilde{g}_{hWW}|^2 \tag{36}$$

where F_0 and F_1 are loop functions associated to scalar and vector bosons, and explicit expressions can be found in ref. [16]. They are a function of $\tau_i = 4m_i^2/m_f^2$, where $i = H, \Delta, W$. The dimensionless couplings $\tilde{g}_{hHH}$ and $\tilde{g}_{h\Delta\Delta}$ are,

$$\tilde{g}_{hHH} = \frac{m_W}{g m_{H^+}^2}\lambda(h_f H^+ H^-)\,, \qquad \tilde{g}_{h\Delta\Delta} = \frac{m_W}{g m_{\Delta^{++}}^2}\lambda(h_f \Delta^{++}\Delta^{--}) \tag{37}$$

where in the fermiophobic case with $O_R^{11} \neq 0$ we find,

$$\lambda(h_f H^+ H^-) \approx \lambda(h_f \Delta^{++} \Delta^{--}) \approx O_R^{11} \beta_3 v_1 \tag{38}$$

up to terms of $\mathcal{O}(v_3)$. In the fermiophobic case with Majoron suppression scenario, where $O_R^{11} = 0$, the terms that were sub-leading in the previous case, dominate now,

$$\begin{aligned} \lambda(h_f H^+ H^-) &\approx 2\lambda_2 v_3 \\ \lambda(h_f \Delta^{++} \Delta^{--}) &\approx 2(\lambda_2 + \lambda_4 - \frac{1}{2}\lambda_5) v_3 \end{aligned} \tag{39}$$

which translate into a diminished influence of the charged scalars in the decay rate for $h_f \to \gamma\gamma$. The other contribution to $h_f \to \gamma\gamma$ is from the W loop, controlled by the dimensionless coupling $\tilde{g}_{hWW}$, which satisfies in both scenarios:

$$\tilde{g}_{hWW} = \frac{1}{g\, m_W} \lambda(h_f W^+ W^-) = \frac{g O_R^{13} v_3}{m_W} \tag{40}$$

This implies that in the case of fermiophobia with Majoron suppression all the contributions from W loops to $\Gamma(h_f \to \gamma\gamma)$ are suppressed.

V. PHENOMENOLOGY OF A HTM FERMIOPHOBIC HIGGS BOSON

In the SM the main Higgs boson decay channels are $h \to b\bar{b}$ and $h \to \tau^+\tau^-$ (for $m_h \leq 130$ GeV). In fermiophobic models though, like the ones based on the 2HDM Type I or the HTM, the fermionic decays are suppressed. As a consequence, decay channels into gauge bosons become the most important ones, including the one-loop generated decays $h \to \gamma\gamma$ and $h \to \gamma Z$. Here we study the decay rates of a fermiophobic Higgs boson into gauge bosons in our HTM, including decay modes with Majorons. For an analysis in the 2HDM see [17, 18]. In the left frame of Fig. 7 we show the fermiophobic Higgs boson branching ratios $B(h_f \to XY)$ as a function of its mass m_f, which include four gauge bosons modes: $\gamma\gamma$, ZZ, WW, and γZ, and modes with one or two Majorons: JJ and JZ. We randomly vary the parameters in the potential as indicated in eq. (24), imposing exact fermiophobia with Majoron suppression via eq. (33). We also use the following experimental restrictions for the Higgs masses,

$$m_{H^\pm} > 80\,\text{GeV}, \quad m_{\Delta^{\pm\pm}} > 136\,\text{GeV}, \quad m_h > 90\,\text{GeV} \quad \text{and} \quad m_A > 90\,\text{GeV}.$$

We highlight from the left frame of Fig. 7 three distinctive features: (i) decay modes with Majorons are very important for low Higgs masses; (ii) decay modes with two massive gauge bosons can dominate for large masses, with a distinctive ratio $B(h_f \to WW)/B(h_f \to ZZ)$ as compared with the SM; (iii) radiative decays are suppressed with the exception of $\gamma\gamma$ at very low masses.

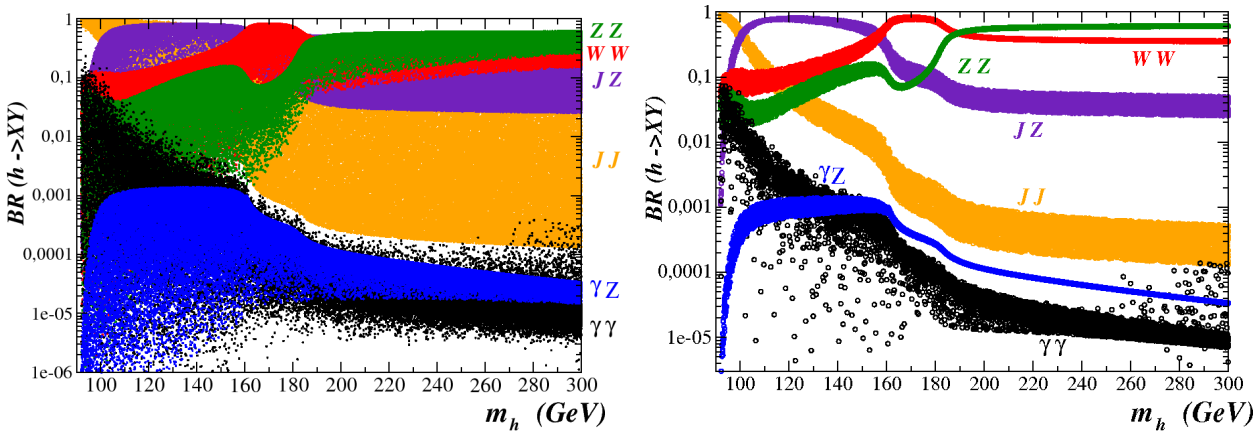

FIG. 7: *Branching ratios for the two-body fermiophobic Higgs decays $h_f \to XY$ as a function of m_f in the fermiophobic scenario with the Majoron suppression approximation. In the left frame parameters are varied freely, while in the right frame they are restricted as indicated in the text.*

In the right frame of Fig. 7 we restrict a few of the free parameters in order to better visualize the above features. The dispersion of allowed points in parameter space is reduced by imposing $700 < v_1 < 1000$ GeV and $\beta_3 < 0.3$.

In the case of the aforementioned feature (i), we see in the left frame that the decay mode $h_f \to JJ$ can dominate at masses $m_f < 160$ GeV, while it becomes smaller than 10% for $m_f \gtrsim 110$ GeV in the restricted case in the right frame. This decay is invisible, since the Majoron escapes detection. Its effect would show up as a diminished production cross section for the visible decays of h_f. The decay mode $h_f \to JZ$ is also very important, and manifests itself as a Z decaying into two fermions plus missing energy. In the restricted case in the right frame, $h_f \to JZ$ dominates for masses $102 < m_f < 155$ GeV, being reduced to a few percent for large Higgs masses.

Regarding feature (ii), both decay modes $h_f \to WW, ZZ$ are above 5% for masses $m_f > 190$ GeV, while in the restricted case (right frame) the two branching ratios are larger than 5% for even smaller masses ($m_f > 130$ GeV). It is also very interesting to note that the decay $h_f \to ZZ$ can have a branching ratio larger than $h_f \to WW$, in contrast with the SM where $B(h_f \to WW)/B(h_f \to ZZ) \approx 2.5$. This situation appear for $m_f > 190$ GeV in the right frame of Fig. 7. In the restricted case, the two branching ratios interchange dominance around $m_f \sim 190$ GeV. This is a very important feature of the model since it can differentiate it from other models. The reason for this behavior lies in the Higgs boson couplings to gauge bosons, and can be understood from eq. (29).

For feature (iii) we see in the left frame of Fig. 7 that the radiatively generated decay $h_f \to \gamma\gamma$ can be potentially important at the LHC ($\gtrsim 6\%$) only for very low Higgs masses $m_h \lesssim 107$ GeV, while the $Z\gamma$

TABLE III: HTM parameters for four scenarios.

Parameter	Scenario 1	Scenario 2	Scenario 3	Scenario 4	Scenario 5	Units
v_1	639.54	931.26	919.58	950.94	862.93	GeV
v_3	0.29	0.13	0.026	0.34	0.072	GeV
λ_1	0.85	2.53	2.81	1.78	2.24	-
λ_2	3.98	3.45	2.86	0.72	-0.86	-
λ_3	0.68	2.90	1.81	1.11	1.36	-
λ_4	2.72	2.54	0.90	-1.68	-0.38	-
λ_5	-0.37	-2.62	-1.52	0.87	1.10	-
β_1	0.45	0.17	0.20	0.27	3.58	-
$\tan(2\theta)$	-0.3	-1.25	1.1	-0.34	-0.015	-
m_h	96.55	92.40	95.18	244.78	272.33	GeV
$m_{H^\pm}$	122.18	219.57	178.89	216.06	239.98	GeV
$m_{\Delta^{\pm\pm}}$	143.29	296.46	234.40	182.89	202.53	GeV
m_A	96.44	94.27	94.81	244.78	272.33	GeV
$hH^\pm H^\mp$	-3.98	1.97	-2.33	0.95	-0.26	GeV
$h\Delta^{\pm\pm}\Delta^{\mp\mp}$	-2.30	0.93	-0.14	-0.49	-0.12	GeV
hWW	-0.12	0.57×10^{-1}	-0.11×10^{-1}	-0.14	3.05×10^{-2}	GeV
hZZ	-0.31	0.15	-0.27×10^{-1}	-0.36	7.78×10^{-2}	GeV
hJJ	-0.33×10^{-2}	0.66×10^{-3}	-0.14×10^{-3}	-1.12×10^{-2}	3.60×10^{-3}	GeV
hZJ	0.33×10^{-3}	-0.11×10^{-3}	0.21×10^{-4}	2.61×10^{-4}	-6.15×10^{-5}	-

mode is irrelevant with a largest value of $\sim 0.1\%$ at intermediate masses $105 \lesssim m_f \lesssim 160$ GeV. These results can also be seen in the restricted case in the right frame.

As we mentioned, one characteristic of our model is that the ratio $B(h_f \to ZZ)/B(h_f \to WW)$ can be larger than unity, while in fermiophobic 2HDM and in the SM, it is smaller than unity. From eq. (29) we see that if the triplet vev vanishes we recover the SM ratio. On the other hand, with exact fermiophobia where $O_R^{12} = 0$ we get an inverted ratio with respect to the SM one. The obvious question is how much deviation from exact fermiophobia is needed to reestablish the SM limit. A similar question is by how much the visible branching ratios change when we deviate from the scenario of exact Majoron suppression. We explore these issues in the following figures.

We define five scenarios in order to explore the effects from deviating from exact fermiophobia and

Majoron suppression. The choice of parameters is random with the following exception: the first three scenarios are chosen such that the decay $h_f \to \gamma\gamma$ is enhanced, and the last two are chosen such that $B(h_f \to ZZ) > B(h_f \to WW)$ for large Higgs masses, in contrast to the SM prediction.

The first three scenarios are characterized by a small fermiophobic Higgs mass, while the last two by a large one. Another difference between them is that in the first three scenarios $m_{H^\pm} < m_{\Delta^{\pm\pm}}$ as opposed to the last two where $m_{H^\pm} > m_{\Delta^{\pm\pm}}$. This can be easily explained using eq.(25). The five scenarios are defined in Table III.

Each scenario, defined by $O_R^{12} = O_R^{11} = 0$, is analyzed in the next five figures. In the left frames we explore the effects of deviation from exact fermiophobia, taking $O_R^{12} \gtrsim 0$. In the right frames we explore the effects of deviation from exact Majoron suppression, taking $O_R^{11} \gtrsim 0$. In Fig. 8 we consider scenario 1. The

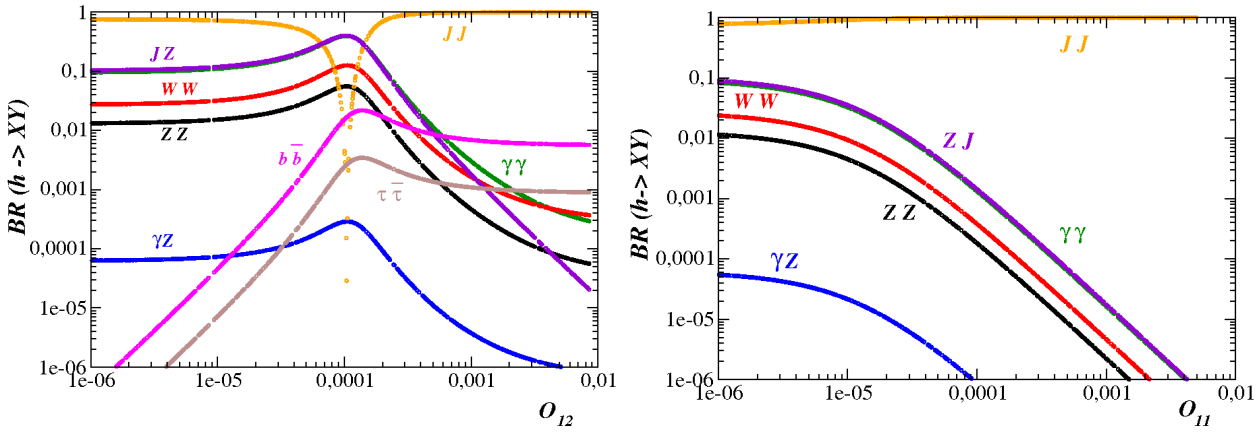

FIG. 8: *Higgs branching ratios for scenario 1, with $m_f = 96.55$ GeV. Deviation from exact fermiophobia in the left frame, and deviation from exact Majoron suppression in the right frame.*

enhancement of the decay $h_f \to \gamma\gamma$ is achieved by choosing a light Higgs boson, which in scenario 1 is $m_h = 96.55$ GeV. The relevant BR are $B(h_f \to \gamma\gamma)$ and $B(h_f \to JZ)$, and they are close to 10% for exact fermiophobia and Majoron suppression, with the invisible mode $B(h_f \to JJ)$ dominating. Deviation from exact fermiophobia is seen in the left frame: both $B(h_f \to \gamma\gamma)$ and $B(h_f \to JZ)$ grow up to 40% because the $h_f JJ$ coupling vanishes when $O_R^{12} \approx 0.0001$. After that, they decrease sharply. The effect of deviation from exact Majoron suppression is seen in the right frame: all visible decay modes diminish rapidly with increasing O_R^{11}. In Fig. 9 we have scenario 2, also with a low Higgs mass of $m_f = 92.4$ GeV. In this case the coupling $h_f JJ$ does not vanish and all bosonic decay modes decrease monotonically, while the fermionic ones increase. In particular, $B(h_f \to \gamma\gamma) \approx 7\%$ for $O_R^{12} = 0.0001$. The behavior of the BR as a function of O_R^{11} is similar to the previous case. Scenario 3 is analyzed in Fig. 10. This is the third scenario with a low Higgs mass, $m_h = 95.18$ GeV, which enhances the decay $h_f \to \gamma\gamma$. This scenario is characterized by

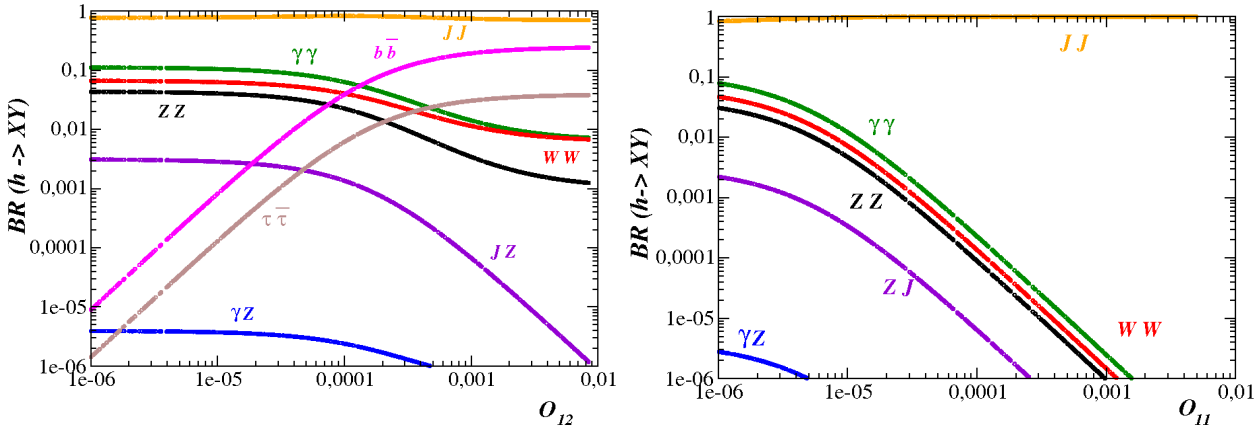

FIG. 9: *Higgs branching ratios for scenario 2, with $m_f = 92.4$ GeV. Deviation from exact fermiophobia in the left frame, and deviation from exact Majoron suppression in the right frame.*

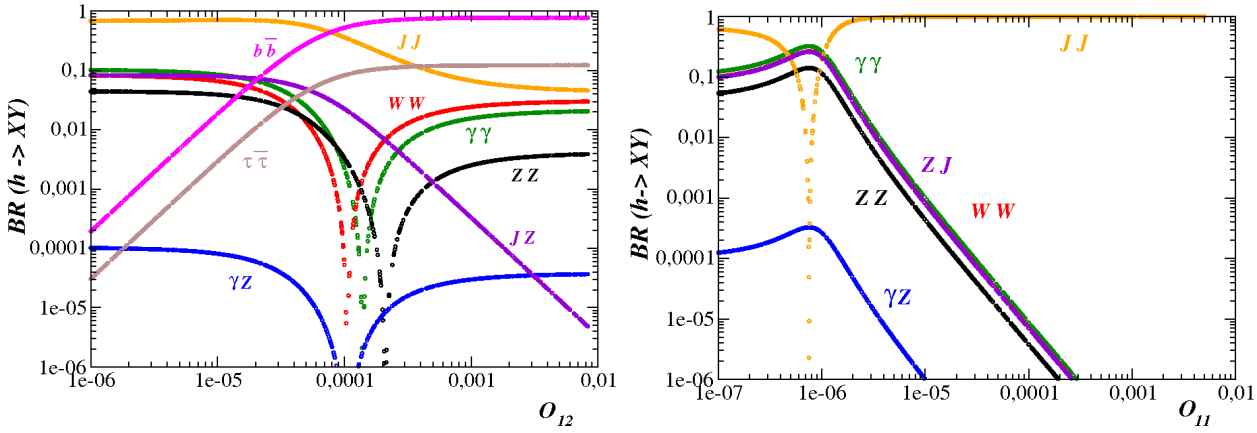

FIG. 10: *Higgs branching ratios for scenario 3, with $m_f = 95.18$ GeV. Deviation from exact fermiophobia in the left frame, and deviation from exact Majoron suppression in the right frame.*

the fact that all Higgs couplings to a pair of gauge bosons vanish at some point in the displayed parameter space. One effect is that the Higgs decay into gauge bosons survives up to higher values of O_R^{12}, for example $h_f \to \gamma\gamma \approx 2\%$ for $O_R^{12} = 0.01$, too small for the LHC, but useful for the ILC. In the right frame we see that the coupling $h_f JJ$ vanishes for $O_R^{11} \approx 7 \times 10^{-7}$, with the effect that visible decay modes increase their branching ratio. After this point the decay channels to the visible channels rapidly decrease. In the following two figures we analyze scenarios 4 and 5, characterized by a large Higgs mass, where the decay modes $h_f \to ZZ$ and $h_f \to WW$ are very important. In Fig. 11 we have scenario 4, characterized by $m_f = 244.78$ GeV. In the left frame we see that the decay modes $h_f \to ZZ$ and $h_f \to WW$ remain between 30% and 70% when we deviate from fermiophobic limit, even up to $O_R^{12} \lesssim 0.01$. In addition, we

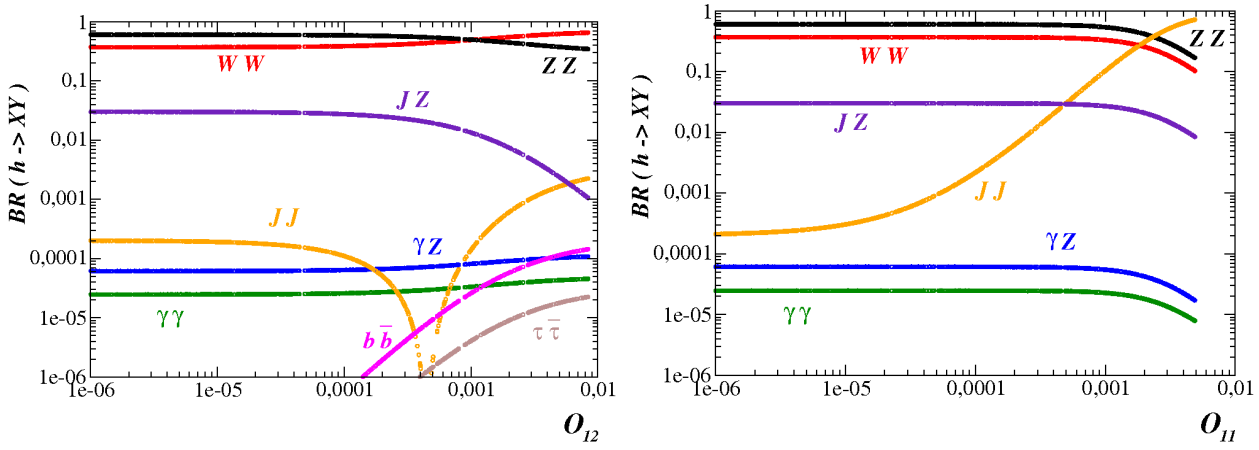

FIG. 11: *Higgs branching ratios for scenario 4, with* $m_f = 244.78$ *GeV. Deviation from exact fermiophobia in the left frame, and deviation from exact Majoron suppression in the right frame.*

see that $B(h_f \to ZZ) > B(h_f \to WW)$ up to $O_R^{12} \approx 0.001$, while for larger values of O_R^{12} the ratio returns to the SM one. In the right frame, one see that the deviation from exact Majoron suppression causes the BR of the decay mode $h_f \to JJ$ to increase until it becomes the largest one for $O_R^{11} \gtrsim 0.002$. However, $B(h_f \to ZZ)$ and $B(h_f \to WW)$ never go below 10% in the displayed parameter space.

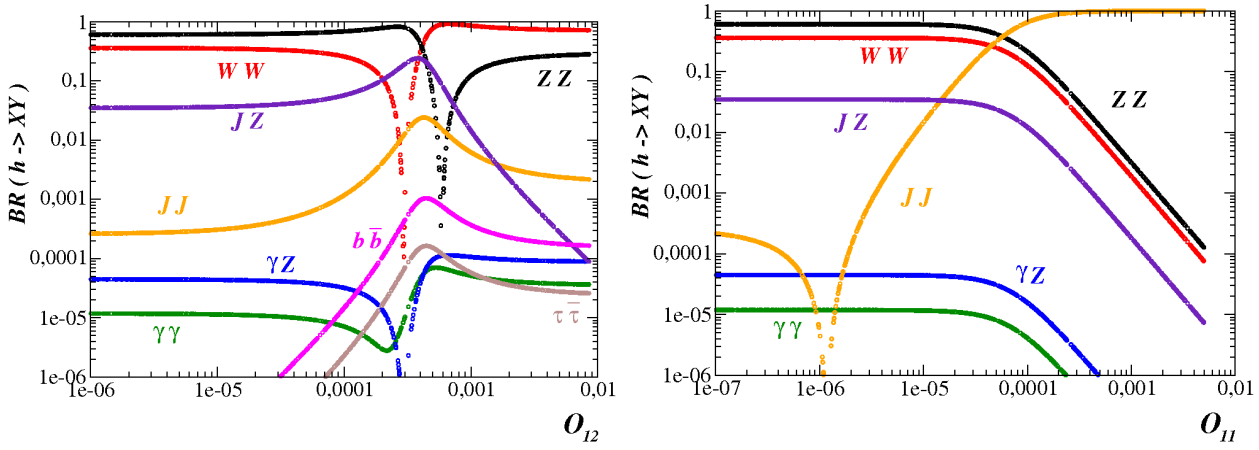

FIG. 12: *Higgs branching ratios for scenario 5, with* $m_f = 272.33$ *GeV. Deviation from exact fermiophobia in the left frame, and deviation from exact Majoron suppression in the right frame.*

The last scenario 5, characterized by $m_f = 272.33$ GeV, is shown in Fig. 12. We see in the left frame that the deviation from exact fermiophobia causes the couplings $h_f WW$ and $h_f ZZ$ to vanish for $O_R^{12} \approx 0.0003$ and $O_R^{12} \approx 0.0006$, respectively. The invisible decay peaks up to 2% between these zeros, but both $B(h_f \to ZZ)$ and $B(h_f \to WW)$ never fall simultaneously below 30%. In the right frame we see that $B(h_f \to ZZ)$ and $B(h_f \to WW)$ remain fairly stable at 60% and 30% respectively when one

deviates from exact Majoron suppression, until $h_f \to JJ$ becomes equally important at $O_R^{11} \approx 5 \times 10^{-5}$. After that point, WW and ZZ modes fall fast, reaching 5% at $O_R^{11} \approx 0.0002$.

We remind the reader that Table I shows that 30% of the allowed parameter space satisfies fermiophobia to a level of $|O_R^{12}| < 0.0014$, and that Table II indicates that 36.6% of parameter space satisfy fermiophobia and Majoron suppression to a level of $|O_R^{13}| > 0.99999$. These numbers tell us that the model "prefers" fermiophobia and/or Majoron suppression, which in turn comes from the hierarchy of the three vacuum expectation values.

VI. CONCLUSIONS

We have studied the Higgs sector of a model with scalar fields in singlet, doublet and triplet isospin representations. In this model the singlet scalar field acquires a vacuum expectation value, which spontaneously breaks lepton number and leads to a vacuum expectation value for the scalar triplet field, the latter providing a mass for the neutrinos. The lightest neutral CP-even scalar (H) can be a fermiophobic Higgs boson (i.e. a scalar with very suppressed couplings to fermions). We have studied distinctive signals of fermiophobia which can be probed at the LHC, and we have shown that fermiophobia is not a fine-tuned situation, unlike in Two Higgs Doublet Models. Characteristic signals are possible for both the cases of small and heavy Higgs boson mass. For a light fermiophobic Higgs boson a distinctive signal would be a moderate $B(H \to \gamma\gamma)$ accompanied by a large $B(H \to JJ)$ (where J is a Majoron), the latter being an invisible decay. For the case of a large Higgs boson mass the decay modes $H \to ZZ, WW$ can be dominant, while the channel $H \to JJ$ is suppressed. In this situation, $B(H \to ZZ)$ is larger than $B(H \to WW)$, which differs from the SM prediction and provides a test for the model.

Appendix A

Here we present the relevant Feynman rules which involve the lightest Higgs boson in our HTM. The notation used here is the same as that used in section II.

Higgs-Higgs-Higgs Interactions

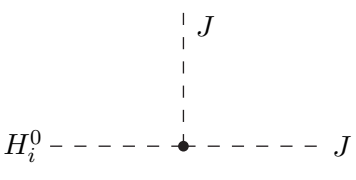

$$
\begin{aligned}
& i\left(O_R^{i1}\left[(O_I^{11})^2 v_1\beta_1 + \tfrac{1}{2}(O_I^{12})^2(v_3\kappa + v_1\beta_2) + \tfrac{1}{2}(O_I^{13})^2 v_1\beta_3 + \right.\right. \\
& O_I^{12}O_I^{13}v_2\kappa\big] + O_R^{i2}\left[\tfrac{1}{2}(O_I^{11})^2 v_2\beta_2 + \tfrac{1}{2}(O_I^{13})^2 v_2(\lambda_5+\lambda_3) + \right. \\
& (O_I^{12})^2 v_2\lambda_1 + \kappa(v_1 O_I^{12}O_I^{13} + v_2 O_I^{11}O_I^{13} + v_3 O_I^{11}O_I^{12})\big] + \\
& O_R^{i3}\left[\tfrac{1}{2}(O_I^{11})^2 v_3\beta_3 + \tfrac{1}{2}(O_I^{12})^2(v_1\kappa + v_3(\lambda_5+\lambda_3)) + v_2\kappa O_I^{11}O_I^{12} + \right. \\
& \left.\left.\left.(O_I^{13})^2 v_3(\lambda_2+\lambda_4)\right]\right)
\end{aligned}
$$

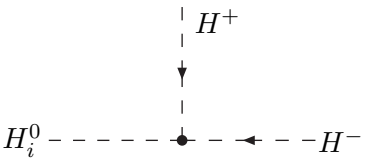

$$i\left(O_R^{i1}\left(s_+^2\beta_3 v_1 - \sqrt{2}s_+c_+\kappa v_2 + c_+^2\beta_2 v_1\right) + O_R^{i2}\left(s_+^2(\lambda_3+\tfrac{1}{2}\lambda_5)v_2 - \tfrac{1}{2}\sqrt{2}s_+c_+(2\kappa v_1 - \lambda_5 v_3) + 2c_+^2\lambda_1 v_2\right) + O_R^{i3}\left(2s_+^2(\lambda_2+\lambda_4)v_3 + \tfrac{1}{2}\sqrt{2}s_+c_+\lambda_5 v_2 + c_+^2\lambda_3 v_3\right)\right)$$

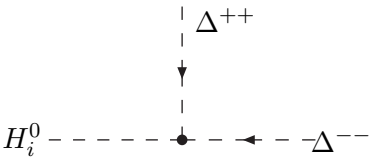

$$i\left(O_R^{i1}\beta_3 v_1 + O_R^{i2}\lambda_3 v_2 + 2O_R^{i3}\lambda_2 v_3\right)$$

Higgs-gauge boson-Higgs Interactions

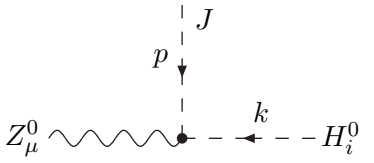

$$ic\,v_2\,v_3\sqrt{g^2+g'^2}(v_3O_R^{i2} - v_2O_R^{i3})(p-k)^\mu$$

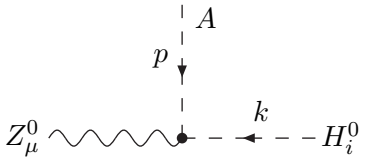

$$i\frac{b}{2v_3}\sqrt{g^2+g'^2}(v_3O_R^{i2} - v_2O_R^{i3})(p-k)^\mu$$

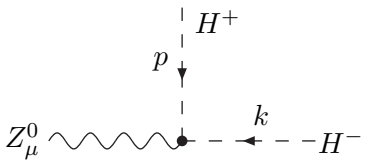

$$i\frac{g'^2(v_2^2+v_3^2) - g^2v_3^2}{\sqrt{g^2+g'^2}(2v_3^2+v_2^2)}(p-k)^\mu$$

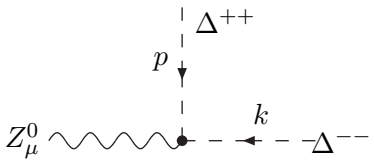

$$-i\frac{g^2-g'^2}{\sqrt{g^2+g'^2}}(p-k)^\mu$$

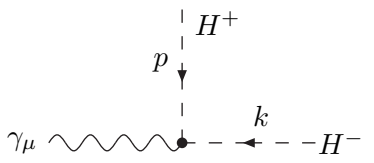

$$-\,i\,e\,(p-k)^\mu$$

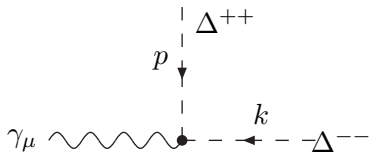

$-2\,i\,e\,(p-k)^\mu$

Higgs-gauge boson-gauge boson Interactions

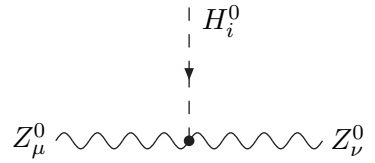

$$i\frac{(g^2+g'^2)}{2}(O_R^{i2}v_2+4O_R^{i3}v_3)g^{\mu\nu}$$

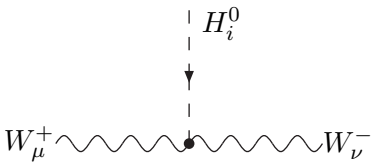

$$i\frac{g^2}{2}(O_R^{i2}v_2+2O_R^{i3}v_3)g^{\mu\nu}$$

Higgs-Higgs- gauge boson-gauge boson Interactions

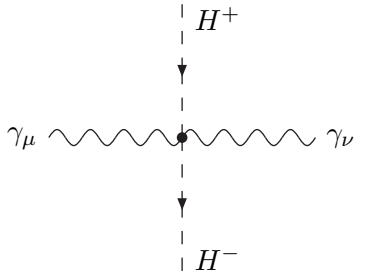

$2\,i\,e^2\,g^{\mu\nu}$

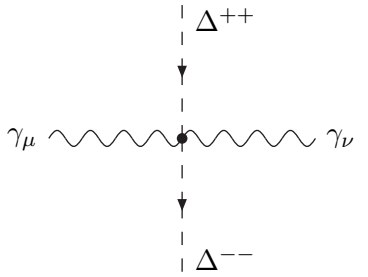

$8\,i\,e^2\,g^{\mu\nu}$

Acknowledgments

A.G.A. was supported by the "National Central University plan to develop first-class universities", and by a Marie Curie Incoming International Fellowship, FP7-PEOPLE-2009-IIF, Contract No. 252263. M.A.D. was supported by Fondecyt Regular Grant # 1100837. M.A.R. was supported by Fondecyt grant No. 3090069. D.R. was supported by CONICYT.

---

[1] R. Barate *et al.* [LEP Working Group for Higgs boson searches and ALEPH Collaboration], the standard model Higgs boson at LEP," Phys. Lett. B **565**, 61 (2003) [arXiv:hep-ex/0306033].

[2] [CDF Collaboration and D0 Collaboration], "Combined CDF and DZero Upper Limits on Standard Model Higgs-Boson Production with up to 4.2 fb-1 of Data," arXiv:0903.4001 [hep-ex].

[3] G. Aad *et al.* [The ATLAS Collaboration], "Expected Performance of the ATLAS Experiment - Detector, Trigger and Physics," arXiv:0901.0512 [hep-ex].

[4] R. Adolphi *et al.* [CMS Collaboration], "The CMS experiment at the CERN LHC," JINST **0803** (2008) S08004 [JINST **3** (2008) S08004].

[5] E. Accomando *et al.*, arXiv:hep-ph/0608079.

[6] H. Georgi and M. Machacek, Nucl. Phys. B **262**, 463 (1985); M. S. Chanowitz and M. Golden, Phys. Lett. B **165**, 105 (1985).

[7] W. Konetschny and W. Kummer, Phys. Lett. B **70**, 433 (1977); T. P. Cheng and L. F. Li, Phys. Rev. D **22**, 2860 (1980); J. Schechter and J. W. F. Valle, Phys. Rev. D **22**, 2227 (1980); R. N. Mohapatra and G. Senjanovic, Phys. Rev. D **23**, 165 (1981).

[8] J. Schechter and J. W. F. Valle, Phys. Rev. D **25**, 774 (1982); P. Fileviez Perez and S. Spinner, Phys. Lett. B **673**, 251 (2009) [arXiv:0811.3424 [hep-ph]].

[9] M. A. Diaz, M. A. Garcia-Jareno, D. A. Restrepo and J. W. F. Valle, Nucl. Phys. B **527**, 44 (1998) [arXiv:hep-ph/9803362].

[10] E. J. Chun, K. Y. Lee and S. C. Park, Phys. Lett. B **566**, 142 (2003); A. G. Akeroyd and M. Aoki, Phys. Rev. D **72**, 035011 (2005); A. G. Akeroyd, M. Aoki and H. Sugiyama, Phys. Rev. D **77**, 075010 (2008); J. Garayoa and T. Schwetz, JHEP **0803**, 009 (2008); M. Kadastik, M. Raidal and L. Rebane, Phys. Rev. D **77**, 115023 (2008); P. Fileviez Perez, T. Han, G. y. Huang, T. Li and K. Wang, Phys. Rev. D **78**, 015018 (2008); F. del Aguila and J. A. Aguilar-Saavedra, Nucl. Phys. B **813**, 22 (2009); A. G. Akeroyd, C. W. Chiang and N. Gaur, arXiv:1009.2780 [hep-ph].

[11] J. F. Gunion, J. Grifols, A. Mendez, B. Kayser and F. I. Olness, Phys. Rev. D **40**, 1546 (1989). K. Huitu, J. Maalampi, A. Pietila and M. Raidal, Nucl. Phys. B **487**, 27 (1997).

[12] T. J. Weiler, "An Overview Of The Higgs Sector With Speculation," *Proceedings of the 8th Vanderbilt Int. Conf. on High Energy Physics, Nashville, TN, Oct 8-10, 1987*; Edited by J. Brau and R. Panvini (World Scientific,

Singapore, 1988), p219.

[13] A. Stange, W. J. Marciano and S. Willenbrock, Phys. Rev. D **49**, 1354 (1994); M. A. Diaz and T. J. Weiler, arXiv:hep-ph/9401259; V. D. Barger, N. G. Deshpande, J. L. Hewett and T. G. Rizzo, arXiv:hep-ph/9211234. In Argonne 1993, Physics at current accelerators and supercolliders* 437-442; H. Pois, T. J. Weiler and T. C. Yuan, Phys. Rev. D **47**, 3886 (1993); A. G. Akeroyd, Phys. Lett. B **368**, 89 (1996); A. Barroso, L. Brucher and R. Santos, Phys. Rev. D **60**, 035005 (1999); L. Brucher and R. Santos, Eur. Phys. J. C **12**, 87 (2000); S. Mrenna and J. Wells, Phys. Rev. D **63**, 015006 (2001); A. G. Akeroyd, M. A. Diaz and F. J. Pacheco, Phys. Rev. D **70**, 075002 (2004); A. G. Akeroyd, Nucl. Phys. B **544**, 557 (1999); A. G. Akeroyd, A. Alves, M. A. Diaz and O. J. P. Eboli, Eur. Phys. J. C **48**, 147 (2006).

[14] M. S. Carena and H. E. Haber, Prog. Part. Nucl. Phys. **50**, 63 (2003) [arXiv:hep-ph/0208209].

[15] D. Phalen, B. Thomas and J. D. Wells, Phys. Rev. D **75**, 117702 (2007); E. Boos, J. C. Brient, D. W. Reid, H. J. Schreiber and R. Shanidze, Eur. Phys. J. C **19**, 455 (2001).

[16] J. F. Gunion, H. E. Haber, G. L. Kane and S. Dawson, "THE HIGGS HUNTER'S GUIDE," Perseus Publishing.

[17] A. G. Akeroyd, M. A. Diaz and M. A. Rivera, Phys. Rev. D **76**, 115012 (2007) [arXiv:0708.1939 [hep-ph]].

[18] A. Arhrib, R. Benbrik, R. B. Guedes and R. Santos, Phys. Rev. D **78**, 075002 (2008).